HHS Public Access

Author manuscript

Adv Mater. Author manuscript; available in PMC 2017 May 01.

Published in final edited form as:

Adv Mater. 2017 February ; 29(7): . doi:10.1002/adma.201604433.

Metal-Organic Framework as a Protective Coating for Biodiagnostic Chips

Congzhou Wang Dr.,
Department of Mechanical Engineering and Materials Science, Institute of Materials Science and Engineering, Washington University in St. Louis, Saint Louis, MO 63130, USA

Sirimuvva Tadepalli,
Department of Mechanical Engineering and Materials Science, Institute of Materials Science and Engineering, Washington University in St. Louis, Saint Louis, MO 63130, USA

Jingyi Luan,
Department of Mechanical Engineering and Materials Science, Institute of Materials Science and Engineering, Washington University in St. Louis, Saint Louis, MO 63130, USA

Keng-Ku Liu,
Department of Mechanical Engineering and Materials Science, Institute of Materials Science and Engineering, Washington University in St. Louis, Saint Louis, MO 63130, USA

Jeremiah J. Morrissey Prof.,
Department of Anesthesiology, Washington University in St. Louis, St. Louis, MO 63110, USA; Siteman Cancer Center, Washington University in St. Louis, St. Louis, MO 63110, USA; Department of Biochemistry and Molecular Biophysics, Washington University in St. Louis, St. Louis, MO 63110, USA; The Center for Clinical Pharmacology, St. Louis College of Pharmacy and Washington, University School of Medicine, St. Louis, MO 63110, USA

Evan D. Kharasch Prof.,
Department of Anesthesiology, Washington University in St. Louis, St. Louis, MO 63110, USA; Siteman Cancer Center, Washington University in St. Louis, St. Louis, MO 63110, USA; Department of Biochemistry and Molecular Biophysics, Washington University in St. Louis, St. Louis, MO 63110, USA; The Center for Clinical Pharmacology, St. Louis College of Pharmacy and Washington, University School of Medicine, St. Louis, MO 63110, USA

Rajesh R. Naik Dr., and
711th Human Performance Wing, Wright-Patterson, Air Force Base, Dayton, OH 45433, USA

Srikanth Singamaneni Prof.
Department of Mechanical Engineering and Materials Science, Institute of Materials Science and Engineering, Washington University in St. Louis, Saint Louis, MO 63130, USA

Antibody–antigen interactions form the basis for various conventional bioassays including enzyme-linked immunosorbent assay,[1] immunoblotting,[2] and immunoprecipitation,[3]

Correspondence to: Rajesh R. Naik, Dr.; Srikanth Singamaneni, Prof..

Supporting Information: Supporting Information is available from the Wiley Online Library or from the author.

owing to their superior binding affinity and selectivity. In recent years, with the rapid development and wide application of biomedical diagnostic tools such as lab-on-a-chip biosensors, antibodies have also been ubiquitously employed as target recognition elements in biosensors with different types of transduction platforms (electrochemical,[4] magnetic,[5] and optical[6]). Unfortunately, as with most proteins, the major limitation of antibodies lies in their poor stability at ambient and elevated temperatures and in nonaqueous media (for instance, on transducer surfaces after immobilization). Thus, antibody-based diagnostic reagents and biosensor chips are required to be maintained under tightly regulated temperature (refrigerated) conditions, to preserve their biofunctionality (recognition capability). This stringent requirement necessitates a temperature-controlled supply chain, the “cold chain”, during transport, storage, and handling of the biodiagnostic reagents and biosensor chips.[7] Apart from causing huge financial and environmental burden, the cold chain system is not always feasible in prehospital and resource-limited conditions such as in urban and rural clinics, developing countries with low-moderate incomes, disaster struck regions, and battle fields, where refrigeration and electricity are not often guaranteed.[8] Therefore, it is imperative to find an alternate approach to preserve the antibody biorecognition capability that relaxes or eliminates the cold chain requirement and increases shelf-life.

Metal-organic frameworks (MOFs), consisting of metal ions or clusters linked by organic ligands,[9] have received increased scientific and technological interest due to their large surface area, tunable porosity, and organic functionality, as well as high thermal stability.[10] These attractive properties render MOFs promising materials for a variety of applications in gas storage,[11] drug delivery,[12] catalysis,[13] and chemical sensors.[14] Within the different emerging applications, a recent study demonstrated the encapsulation of a wide range of biomolecules within MOFs by growing them in the presence of the biomolecules under mild biocompatible conditions (e.g., aqueous solution at room temperature).[15] More importantly, with the protection of the MOF layer, the activity of encapsulated biomolecules (such as enzymes) could be preserved against different extreme environmental conditions including high temperatures and organic solvents. This work demonstrated the preservation of biocatalytic activity of enzymes in solution. We hypothesize that MOFs can be a powerful class of materials for preserving the biorecognition capability of antibodies immobilized on biosensor surfaces, considering that the MOFs can be adapted to grow on different substrates (films, particles, and gels).[16,17]

In this study, we demonstrate MOF coatings to be highly effective in preserving the biorecognition capabilities of antibodies immobilized on sensor surfaces that are exposed to elevated temperatures. In contrast to previous approaches that involve mixing protein (enzyme) with MOF precursors in solution, a zeolitic imidazolate framework-8 (ZIF-8) was grown on bionanoconjugates immobilized on gold nanorods. Just before using the biochip, a simple aqueous rinsing step completely removed the MOF protective layer, restoring the biofunctionality of the sensor surface (Figure 1). Owing to the high sensitivity, cost-efficiency and great potential of use in point-of-care (POC) diagnostics,[18] a plasmonic nanobiosensor based on refractive index sensitivity of localized surface plasmon resonance (LSPR) is used as the platform to monitor various fabrication stages including conjugation of the antibody to the surface of the plasmonic nanostructures, formation and removal of the

MOF, as well as bioanalyte detection. Proof-of-concept is initially established by employing IgG/anti-IgG as a test system, showing that the MOF layer remarkably improves the stability of the model antibody at room temperature, 40 and 60 °C. The biopreservation efficiency of MOFs is found to be higher than the previously reported silk-based approach.[19] We also demonstrate that this approach can be applied to increase the shelf-life and thermal stability of a bioplasmonic paper device designed for the detection of neutrophil gelatinase associated lipocalin (NGAL), a urinary biomarker for acute kidney injury and chronic kidney disease in resource-limited settings. Overall, by eliminating the cold chain requirement in transportation, storage, and handling through an environmentally friendly and energy-efficient method, this novel approach paves the way for antibody-based biosensors in prehospital, point-of-care, and resource-limited circumstances such as ambulance, developing countries, battlefield, and the patient's home.

Rabbit IgG and goat anti-rabbit IgG (termed IgG and anti-IgG henceforth) were employed as model antibody and bioanalyte, respectively, to establish the proof-of-concept. Here, gold nanorods (AuNRs) were used as plasmonic nanotransducers for label-free sensing because of their large refractive index sensitivity and excellent tunability of the LSPR wavelength.[20] We synthesized AuNRs with a length of 48.2 ± 1.8 nm and a diameter of 18.2 ± 1.1 nm using a seed-mediated approach (Figure 2A).[21] As described earlier,[20] the conjugation of the antibody (IgG) to AuNRs is achieved by conjugating IgG molecules to a bifunctional polyethylene glycol (COOH-PEG-SH) chain and subsequently attaching the formed IgG-PEG-SH onto the AuNRs surface through gold-thiol linkage. The polyethylene glycol (PEG) chain acts as a flexible spacer, increases the accessibility of target biomolecules to IgG and also serves as a stable protective layer around the AuNRs to minimize nonspecific binding. After conjugating IgG onto the AuNRs surface, the longitudinal LSPR wavelength of the AuNRs showed a 7.5 nm redshift due to the increase in the refractive index of the medium surrounding the AuNR (Figure 2B). These AuNR-IgG conjugates were then immobilized onto the 3-mercaptopropyl-trimethoxysilane-functionalized glass surfaces. To probe the sensing capability of the plasmonic nanobiosensor, the substrates were exposed to different concentrations of anti-IgG leading to specific binding to IgG, which can be quantified by the redshift in the LSPR wavelength of the AuNRs. We observed a monotonic increase in the LSPR shift with an increasing concentration of the anti-IgG. The limit of detection was found to be 240 pg mL^{-1} (Figure 2C), consistent with our previous reports.[19] Considering that the LSPR wavelength redshifted maximally by 15.5 nm at the highest concentration (24 μg mL^{-1}) of anti-IgG (Figure 2D), in the following experiments we have employed 24 μg mL^{-1} of anti-IgG to quantify the biorecognition capability of the antibody (IgG) subjected to different storage conditions.

A MOF has been previously used in encapsulating an enzyme and providing thermal stability.[22] The preservation mechanism is attributed to the small pore size of the MOF and coordination interactions between the carbonyl groups of the protein backbone and the Zn cations of ZIF-8, providing proteins with tight encapsulation.[15,23] In this study, we posit that a MOF coating on a biosensor surface would protect the biorecognition capability of the underlying antibody. In addition to the detection and quantification of target analytes, refractive index sensitivity of the LSPR wavelength of the AuNRs can also be exploited to monitor the formation and removal of the MOF coating (Figure 3A,B). After immersing the

biochips with immobilized AuNR-IgG into the MOF precursor solution (a mixture of 2-methylimidazole and zinc acetate) for 3 h, the LSPR wavelength exhibited a ≈30 nm redshift (step 2 in Figure 3B), suggesting the formation of a MOF coating on top of the AuNR-IgG conjugates. Interestingly, immersing the bare AuNRs-immobilized glass substrate into the MOF precursor solution for 3 h resulted in a LSPR wavelength shift of only ≈2 nm possibly due to the adsorption of the MOF precursors on the AuNR or extremely slow growth of ZIF-8 on the bare AuNR (Figure S1, Supporting Information). This is in stark contrast with the rapid growth of ZIF-8 on bioconjugated nanostructures.[16] After storing the MOF-coated plasmonic biochips at the desired temperature and duration, the MOF protective coating can be quickly removed by rinsing the biochip with distilled water at pH 6. The complete removal of the MOF is evidenced by a ≈30 nm blueshift in the LSPR wavelength (step 3 in Figure 3B). It is important to ensure complete removal of the MOF protective coating and restoration of the biorecognition capability of the biosensor before exposing the plasmonic biochips to the analyte solution. Subsequently (step 4 in Figure 3B), the restored biochip displayed a 14 nm redshift upon specific binding of anti-IgG (24 μg mL^{-1}) to IgG. The percentage of retained recognition capability (%) was used to quantitatively evaluate the antibody preservation efficacy of the MOF under various storage conditions. The retained recognition capability was calculated as the percentage of the redshift upon specific binding of anti-IgG (24 μg mL^{-1}) to IgG on a restored biochip after several days of storage at elevated temperatures compared with the redshift obtained from the same batch of freshly made substrate (which was considered as the reference sample tested instantly without a MOF coating). For example, the redshift of 14 nm compared with the redshift of 16 nm in the case of the reference sample in the same batch corresponds to a retained recognition capability of 87.5% (Figure 3A,B). Therefore, ≈88% recognition capability of the antibody-based biochip was found to be preserved after two days of storage at room temperature.

The MOF film formation and removal was further confirmed by atomic force microscope (AFM) imaging. Prior to incubating the substrate with the MOF precursor solution, the AuNR-IgG conjugates were found to be uniformly distributed on the substrate (Figure 3C). After the coating process, the AuNR-IgG conjugates were found to be covered by the MOF film that exhibited dense grainy morphology (Figure 3D). This is further confirmed by the scanning electron microscope (SEM) images (Figure S2, Supporting Information). After rinsing the substrate with water at pH 6, the AuNR-IgG conjugates were exposed without any MOF residue on the substrate (Figure 3E). The AFM scratch test indicated the thickness of the MOF film to be ≈50 nm, which is sufficient to completely cover the AuNR-IgG conjugates (≈22 nm height) (Figure S3, Supporting Information). To ascertain that ZIF-8 crystals were formed on the surface of AuNR-IgG conjugates, Fourier transform infrared spectroscopy (FTIR) and X-ray diffraction (XRD) were employed (Figure 3F,G). FTIR spectrum obtained before the formation of the MOF layer exhibited absorption peaks at 1640–1650 and 1520–1530 cm^{-1}, corresponding to amide I and amide II bands of IgG, respectively. After the MOF formation, the FTIR spectrum exhibited new absorption bands corresponding to the MOF apart from the amide I and amide II bands of the protein. The characteristic absorption peak at 1583 cm^{-1} corresponds to the C=N stretching of imidazole and the peak at 1420 cm^{-1} is associated with the imidazole ring stretching.[24] These characteristic absorption bands were also observed in the FTIR spectrum obtained from pure

ZIF-8 (Figure S4A, Supporting Information). Interestingly, the amide I vibrational mode for the MOF-coated AuNR-IgG shifted to higher frequency (from 1643 to 1649 cm^{-1}, Figure S4B, Supporting Information), suggesting the protein–MOF interaction due to the coordination between the Zn cations and the carbonyl group of the proteins.[15] Furthermore, XRD measurements confirmed the formation of ZIF-8 crystals on the top of the AuNR-IgG surface (Figure 3G). The XRD patterns and related peak positions were in agreement with the typical structure of ZIF-8[25] except for the absence of (011) and (112) plane, implying the possible orientation of ZIF-8 formed on the AuNR-IgG immobilized substrate. The XRD pattern also shows a strong peak at 10.88°, indicating the partial orientation of the crystals in (001) direction. It has been previously reported that the surface properties can significantly influence the nucleation and crystal growth of ZIF-8.[26] This suggestion was further confirmed by powder XRD of pure ZIF-8 and ZIF-8 formed in IgG solution, which exhibited all peaks of ZIF-8 including those corresponding to (011) and (112) planes and relatively low intensity peak at 10.88° (Figure S5, Supporting Information).

Before performing a comprehensive investigation of the efficacy of the ZIF-8 layer as protective coating for preserving the antibody recognition capabilities, it is important to determine whether the preservation process itself would compromise the biochip performance. An important aspect that needs to be considered is the effect of ZIF-8 growth and rinsing on the recognition capability of the antibodies conjugated to the plasmonic nanostructures. To address this aspect, we coated the ZIF-8 film onto a freshly made AuNR-IgG immobilized biochip and immediately removed the ZIF-8 film. After incubation of the biochip with the analyte solution containing 24 μg mL^{-1} of anti-IgG, we observed a ≈16 nm redshift, very close to that noted for the reference sample (Figure S6, Supporting Information). The virtually complete preservation of the specific recognition capability of IgG-AuNR conjugates after subjecting the biochip to the preservation process (i.e., the MOF layer growth and removal) indicates that the MOF-based preservation steps do not adversely affect the biochip performance.

Next, we set out to investigate the efficacy of MOF to preserve the biorecognition ability of IgG conjugated to the AuNR upon exposure to harsh conditions (such as high temperatures) that would normally lead to denaturation and loss of recognition capabilities. The plasmonic biochip with and without the MOF coating were stored at room temperature, 40 and 60 °C for one week. To eliminate the influence of relative humidity variations in the standard laboratory environment, all the samples were stored in sealed containers. ZIF-8 has excellent thermal stability (up to 550 °C), as well as chemical resistance to boiling alkaline water and organic solvents.[27] However, it is not stable in acidic environments because of the loss of the coordination between the zinc ions and imidazolate at pH 5.0–6.0.[28] Therefore, as long as ZIF-8 protected surfaces are stored in dry or nonacidic conditions, the ZIF-8 shell should be stable. For the same reason, water at pH 6 was employed to completely remove the ZIF-8 protective layer and restore the biofunctionality of antibodies conjugated to nanotransducers. Different substrates were sampled at selected time intervals (1, 2, 3, and 7 d) to monitor the changes in the biorecognition capability of the antibodies (Figure 4A). Samples with MOF coatings showed only an approximately 20% loss in biorecognition capability after storage at room temperature (25 °C) for one week compared with the nearly complete loss in biorecognition capability for substrates without MOF protective layer. Even at higher

temperatures, 40 and 60 °C, MOF-coated biochips retained over 70% of biorecognition ability after one week. In contrast, substrates without any MOF protective layer lost over 90% of biorecognition capability within the first day at 40 and 60 °C. Furthermore, we selected one storage condition (three days storage at room temperature) and investigated the detection sensitivity (LSPR shift) at varying concentrations of anti-IgG after removal of ZIF-8. The LSPR shifts at different concentrations of anti-IgG were compared with the results from freshly made samples (the results in Figure 2C). Across the entire concentration range tested here, we noted a consistent ≈15 % decrease in LSPR shift (Figure 4B; Figure S7, Supporting Information). The limit of detection of the plasmonic biosensor stored for three days at room temperature is found to be 240 pg mL^{-1} (defining 1 nm as 3σ noise level), which is similar to a freshly prepared biosensor. Compared with our previous approach involving silk fibroin as a protective layer, the MOF coating is vastly superior in terms of biopreservation efficacy, ease of formation and removal, as well as availability and cost of the raw materials.[19] While the silk-coated plasmonic biochips retained a biorecognition capability of ≈40% after one week at 40 °C, the MOF-coated biochips retained over 70% of biorecognition ability under identical storage conditions (Figure 4C). Furthermore, complete removal of the silk film can be difficult if the silk-encapsulated biochips are subjected to harsh conditions such as high temperature or organic solvents, which results in the conversion of silk I to the insoluble silk II state.[29] In addition, both 2-methylimidazole and zinc acetate are commercially available, whereas silk fibroin extraction and purification procedures involve several processing steps that need to be executed with significant caution. Taken together, MOFs are a better choice compared with silk fibroin as the protective layer to stabilize antibody-based biosensors against extreme environments.

Finally, we sought to evaluate the applicability of this approach to clinically relevant biodiagnostic devices. We have previously introduced a bioplasmonic paper device (BPD) as a novel platform for LSPR-based biosensors.[20,30] Compared with conventional rigid substrates such as glass, paper substrates offer numerous advantages such as high surface area, excellent wicking properties, mechanical flexibility, low cost, easy disposability, small sample volume requirement, facile processing (cutting, bending, dipping), and compatibility with conventional printing approaches (enabling multiplexed detection and multimarker biochips). Here, we chose NGAL, a urinary biomarker for acute kidney injury, as the target analyte. Considering that urinary NGAL levels are increased by several log-orders (100-fold to 1000-fold) of magnitude during acute kidney injury, rapid measurement of urine NGAL levels in resource-limited settings is of great clinical importance.[31] The fabrication of BPD for NGAL detection is achieved by the immersion of a 1 cm × 1 cm strip of filter paper in NGAL antibody-conjugated AuNR solution. The SEM images of the paper revealed a uniform distribution of the AuNR-NGAL antibody conjugates with no signs of aggregation or patchiness (Figure 5A). Similar to AuNR-IgG on glass substrates, the coating of the MOF on the paper substrate also induced a ≈30 nm redshift (Figure 5B). After rinsing with distilled water at pH 6, a blueshift of ≈30 nm suggested the complete removal of the MOF from the paper (Figure 5B,C). This is in stark contrast to silk-based preservation, which is not suitable for paper substrates due to the difficulties associated with the removal of the silk film from paper substrates. A time-lapse experiment, similar to the one described above, was performed to monitor the recognition capability of the NGAL antibodies on the paper-based

plasmonic biosensor stored at room temperature and 60 °C (Figure 5D). As expected, the antibody-based BPDs with MOF protective coating retained nearly 80% of recognition capability after storage at both room temperature and 60 °C for one week, while bare BPDs without protective layer quickly lost biorecognition at both temperatures. Apart from the generality of the MOF protection approach, these results demonstrate the feasibility of dramatically enhancing the thermal stability and preserving the recognition capability of a clinically relevant biosensor device, enabling their use in POC and resource-limited settings.

In summary, for the first time, we have demonstrated that MOFs (ZIF-8) can be used as a protective material to preserve the recognition capability of antibodies on biosensor surfaces stored at ambient and elevated temperatures. With the protection of the MOF, both rabbit IgG and anti-NGAL appended to plasmonic biosensors retained over 70% of recognition capability compared with complete loss in unprotected samples after one week of storage at room temperature, 40 and 60 °C. Such antibody-based biosensors with enhanced thermal stability eliminate the need for a cold chain system during transportation and storage in an energy-efficient and environmentally-friendly fashion. Furthermore, the biofunctionality of the MOF-coated biochip can be restored by a simple water rinsing step, making it highly convenient for use in POC and resource-limited settings such as in an ambulance, intensive care unit, emergency room, battlefield, or the developing world. We also demonstrate generality and applicability of this approach to a clinically relevant bioplasmonic paper device, which offers several advantages over rigid substrates. The improved preservation efficiency, ease of implementation (formation and removal), and wide availability of precursors make MOFs vastly superior to our previous silk-based preservation approach. Overall, we expect this facile and low-cost biopreservation method to greatly advance the application of various antibody-based biosensor platforms in POC and resource-limited settings. More broadly, MOFs are expected to be a new class of biopreservation material, playing an important role in realizing ultrastable biodiagnostics and therapeutics for resource-limited settings.

Supplementary Material

Refer to Web version on PubMed Central for supplementary material.

Acknowledgments

The authors acknowledge support from the Air Force Office of Scientific Research (Grant Nos. FA9550-15-1-0228 and 12RX11COR), AFRL/711 HPW, and the National Institutes of Health (Grant Nos. R21DK100759 and R01 CA141521). The authors thank the Nano Research Facility (NRF) at Washington University for providing access to electron microscopy facilities. The authors thank Mr. Qisheng Jiang forhe lp with TEM imaging.

References

1. Johnson AJ, Martin DA, Karabatsos N, Roehrig JT. J Clin Microbiol. 2000; 38:1827. [PubMed: 10790108]
2. Ashley RL, Militoni J, Lee F, Nahmias A, Corey L. J Clin Microbiol. 1988; 26:662. [PubMed: 2835389]
3. Scully R, Chen J, Plug A, Xiao Y, Weaver D, Feunteun J, Ashley T, Livingston DM. Cell. 1997; 88:265. [PubMed: 9008167]

4. Vidal JC, Bonel L, Ezquerra A, Hernandez S, Bertolin JR, Cubel C, Castillo JR. Biosens Bioelectron. 2013; 49:146. [PubMed: 23743326]
5. Ng E, Nadeau KC, Wang SX. Biosens Bioelectron. 2016; 80:359. [PubMed: 26859787]
6. Endo T, Kerman K, Nagatani N, Hiepa HM, Kim DK, Yonezawa Y, Nakano K, Tamiya E. Anal Chem. 2006; 78:6465. [PubMed: 16970322]
7. Zhang J, Pritchard E, Hu X, Valentin T, Panilaitis B, Omenetto FG, Kaplan DL. Proc Natl Acad Sci USA. 2012; 109:11981. [PubMed: 22778443]
8. Wolfson LJ, Gasse F, Lee-Martin SP, Lydon P, Magan A, Tibouti A, Johns B, Hutubessya R, Salama P, Okwo-Bele JM. Bull W H O. 2008; 86:27. [PubMed: 18235887]
9. Yaghi OM, O'Keeffe M, Ockwig NW, Chae HK, Eddaoudi M, Kim J. Nature. 2003; 423:705. [PubMed: 12802325]
10. a) Furukawa H, Cordova KE, O'Keeffe M, Yaghi OM. Science. 2013; 341:974.b) Foo ML, Matsuda R, Kitagawa S. Chem Mater. 2014; 26:310.c) Lu G, Farha OK, Zhang W, Huo F, Hupp JT. Adv Mater. 2012; 24:3970. [PubMed: 22718482]
11. a) Murray LJ, Dinca M, Long JR. Chem Soc Rev. 2009; 38:1294. [PubMed: 19384439] b) Oh Y, Le VD, Maiti UN, Hwang JO, Park WJ, Lim J, Lee KE, Bae YS, Kim YH, Kim SO. ACS Nano. 2015; 9:9148. [PubMed: 26267150]
12. Horcajada P, Serre C, Vallet-Regi M, Sebban M, Taulelle F, Ferey G. Angew Chem Int Ed. 2006; 45:5974.
13. Ma L, Abney C, Lin W. Chem Soc Rev. 2009; 38:1248. [PubMed: 19384436]
14. Kreno LE, Leong K, Farha OK, Allendorf M, van Duyne RP, Hupp JT. Chem Rev. 2012; 112:1105. [PubMed: 22070233]
15. Liang K, Ricco R, Doherty CM, Styles MJ, Bell S, Kirby N, Mudie S, Haylock D, Hill AJ, Doonan CJ, Falcaro P. Nat Commun. 2015; 6:7240. [PubMed: 26041070]
16. Liang K, Carbonell C, Styles MJ, Ricco R, Cui J, Richardson JJ, Maspoch D, Caruso F, Falcaro P. Adv Mater. 2015; 27:7293. [PubMed: 26478451]
17. Zheng G, de Marchi S, López-Puente V, Sentosun K, Polavarapu L, Pérez-Juste I, Hill EH, Bals S, Liz-Marzán LM, Pastoriza-Santos I, Pérez-Juste J. Small. 2016; 12:3953.
18. a) Anker JN, Hall WP, Lyandres O, Shah NC, Zhao J, van Duyne RP. Nat Mater. 2008; 7:442. [PubMed: 18497851] b) Cha SK, Mun JH, Chang T, Kim SY, Kim JY, Jin HM, Lee JY, Shin J, Kim KH, Kim SO. ACS Nano. 2015; 9:5536. [PubMed: 25893844]
19. Wang C, Luan J, Tadepalli S, Liu KK, Morrissey JJ, Kharasch ED, Naik RR, Singamaneni S. ACS Appl Mater Interfaces. 2016; 8:26493. [PubMed: 27438127]
20. Tian L, Chen E, Gandra N, Abbas A, Singamaneni S. Langmuir. 2012; 28:17435. [PubMed: 23163716]
21. a) Lee KS, El-Sayed MA. J Phys Chem B. 2005; 109:20331. [PubMed: 16853630] b) Chen H, Shao L, Li Q, Wang J. Chem Soc Rev. 2013; 42:2679. [PubMed: 23128995]
22. Liang K, Coghlan CJ, Bell SG, Doonan C, Falcaro P. Chem Commun. 2016; 52:473.
23. Feng Y, Schmidt A, Weiss RA. Macromolecules. 1996; 29:3909.
24. a) Hu Y, Kazemian H, Rohani S, Huang Y, Song Y. Chem Commun. 2011; 47:12694.b) Nordin N, Ismail AF, Mustafa A, Goh PS, Rana D, Matsuura T. RSC Adv. 2014; 4:33292.
25. a) Zhu M, Jasinski JB, Carreon MA. J Mater Chem. 2012; 22:7684.b) Eslava S, Zhang L, Esconjauregui S, Yang J, Vanstreels K, Baklanov MR, Saiz E. Chem Mater. 2013; 25:27.
26. Li S, Shi W, Lu G, Li S, Loo SCJ, Huo F. Adv Mater. 2012; 24:5954. [PubMed: 22936521]
27. Park KS, Ni Z, Cote AP, Choi JY, Huang RD, Uribe-Romo FJ, Chae HK, O'Keeffe M, Yaghi OM. Proc Natl Acad Sci USA. 2006; 103:10186. [PubMed: 16798880]
28. a) Zhuang J, Kuo CH, Chou LY, Liu DY, Weerapana E, Tsung CK. ACS Nano. 2014; 8:2812. [PubMed: 24506773] b) Adhikari C, Das A, Chakraborty A. Mol Pharm. 2015; 12:3158. [PubMed: 26196058]
29. Li AB, Kluge JA, Guziewicz NA, Omenetto FG, Kaplan DL. J Controlled Release. 2015; 219:416.
30. Tadepalli S, Kuang Z, Jiang Q, Liu KK, Fisher MA, Morrissey JJ, Kharasch ED, Slocik JM, Naik RR, Singamaneni S. Sci Rep. 2015; 5:16206. [PubMed: 26552720]

31. a) Abbas A, Tian L, Morrissey JJ, Kharasch ED, Singamaneni S. Adv Funct Mater. 2013; 23:1789. [PubMed: 24013481] b) Devarajan P. Nephrology. 2010; 15:419. [PubMed: 20609093]

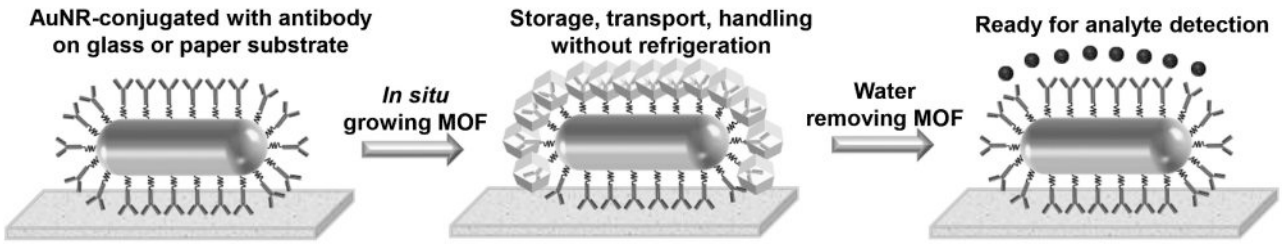

Figure 1.

Schematic illustrating the concept of using MOFs to enhance the thermal stability of antibody-based plasmonic biochips, not only eliminating the need for refrigerated transportation, handling and storage, but also enabling convenient use in resource-limited settings.

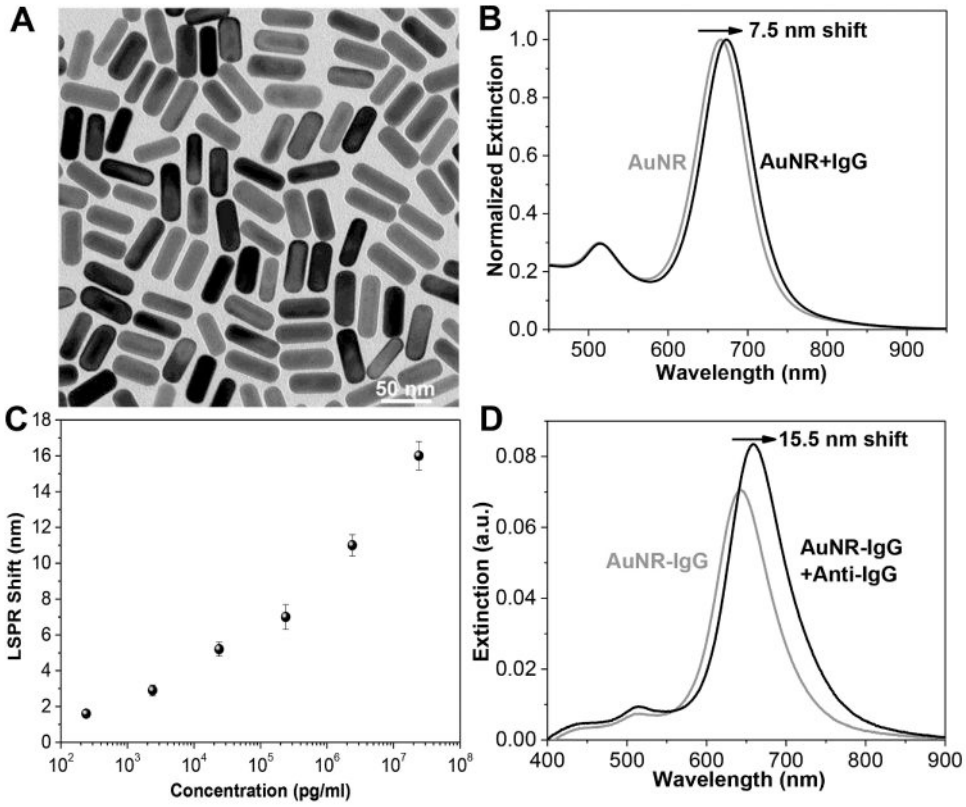

Figure 2.

A) Transmission electron microscopy (TEM) image of AuNRs used as plasmonic nanotransducers. The dimension of the AuNRs is 48×18 nm. B) Extinction spectra showing the LSPR shift after conjugation of AuNR with IgG in solution. The λ_{max} redshifts by 7.5 nm. C) LSPR shift of AuNR-IgG on glass substrate upon exposure to various concentrations of anti-IgG solutions showing the monotonic increase in the LSPR shift with concentration. Error bars represent standard deviations from three different samples. D) Extinction spectra of AuNR-IgG conjugates on the glass substrate before and after exposure to anti-IgG (24 μg mL^{-1}). The λ_{max} redshifts by 15.5 nm.

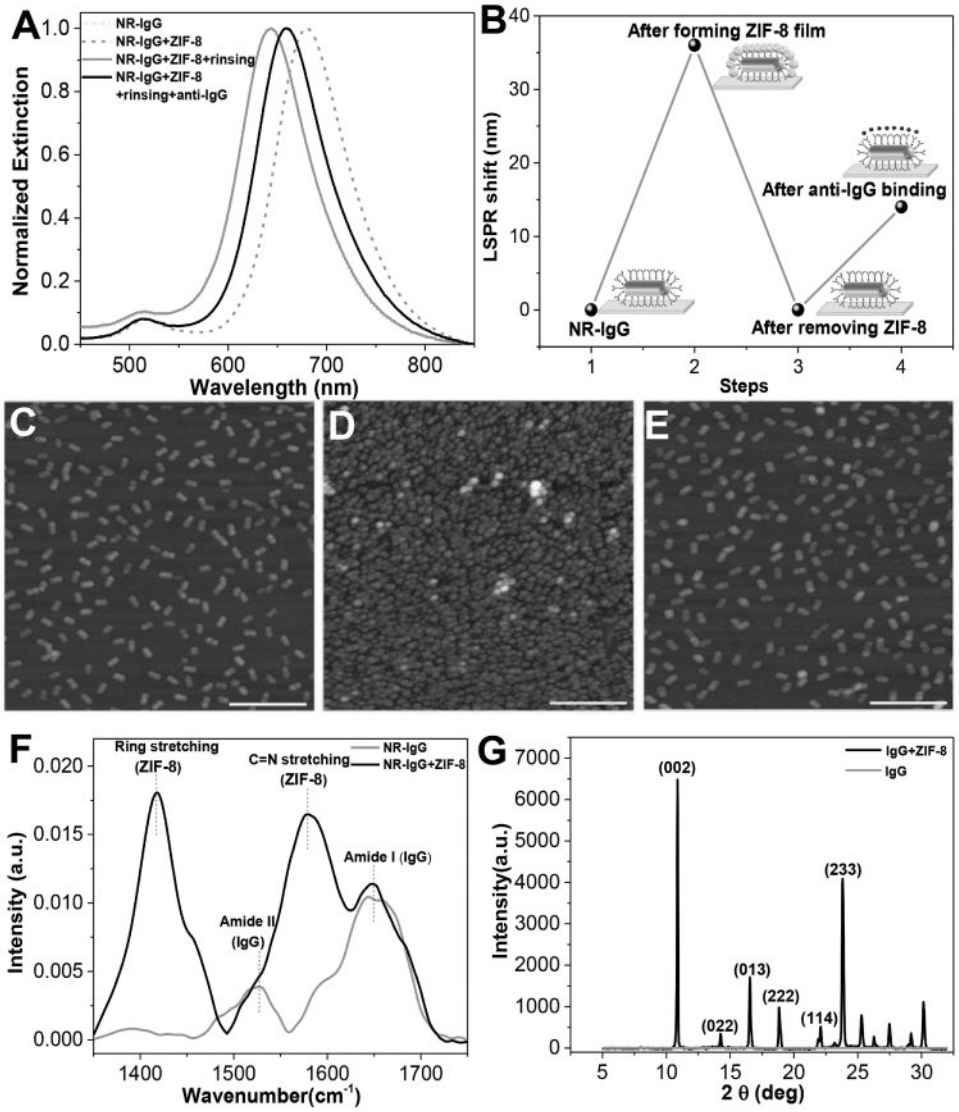

Figure 3.

A) Extinction spectra of AuNR-IgG conjugates on the glass substrate before and after ZIF-8 film coating, after removing ZIF-8 film and after exposure to 24 μg mL^{-1} of anti-IgG. B) LSPR shift corresponding to each step shown in panel (A). AFM images showing C) uniformly adsorbed AuNR-IgG on glass substrate before ZIF-8 film coating, D) AuNR-IgG conjugates covered by ZIF-8 film, and E) complete removal of ZIF-8 after rinsing with distilled water at pH 6. Scale bars: 500 nm. F) FTIR spectra of AuNR-IgG before and after ZIF-8 coating. G) XRD spectra of AuNR-IgG before and after ZIF-8 coating.

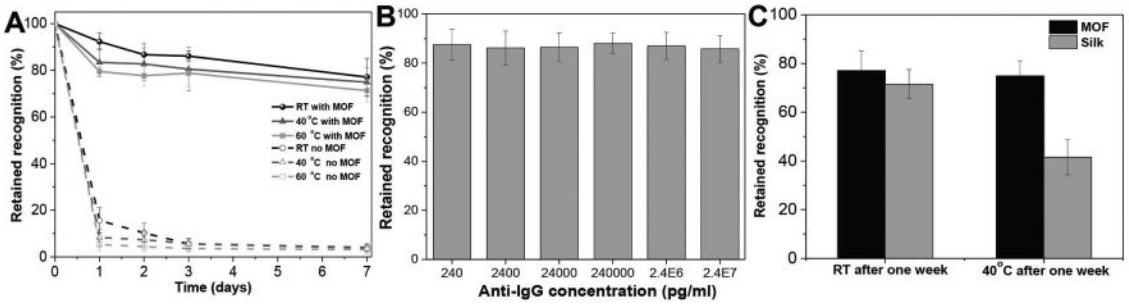

Figure 4.

A) Retained recognition capability of MOF-coated IgG-AuNR conjugates on glass substrates stored at room temperature, 40 and 60 °C for different durations. B) Retained recognition capability of MOF-coated IgG-AuNR conjugates stored at room temperature for three days measured by exposing the substrates to different concentrations of anti-IgG. C) The comparison of preservation efficiency between MOF and silk as the protective materials after one week at room temperature and 40 °C. Error bars represent standard deviations from three independent samples.

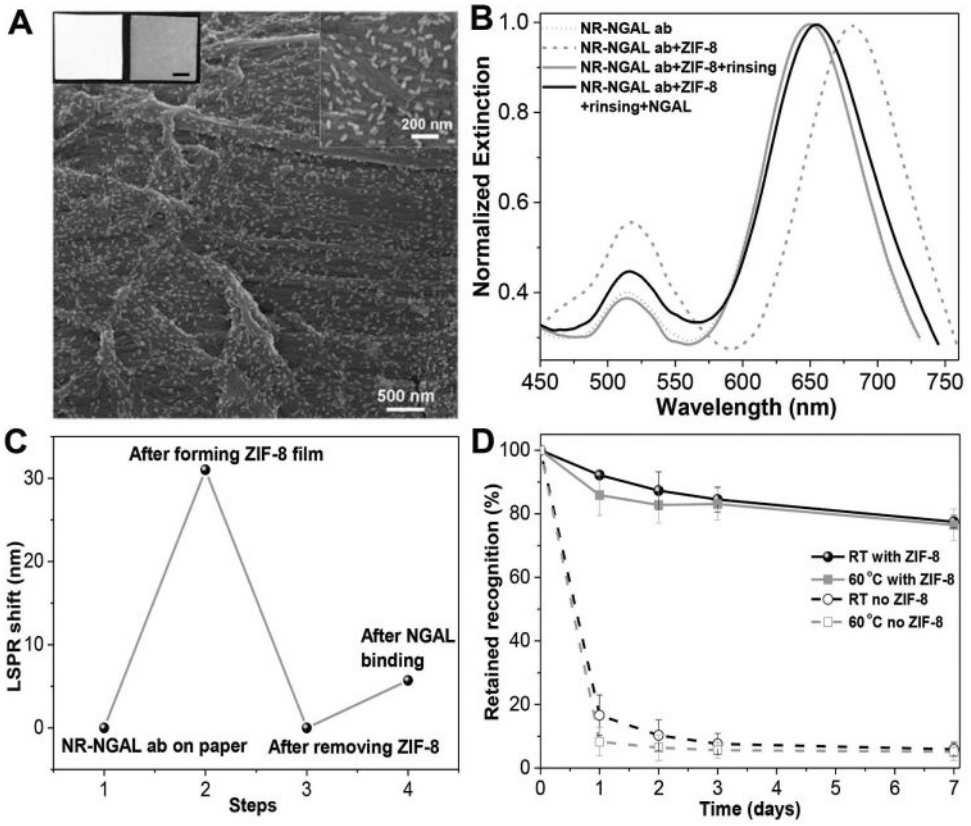

Figure 5.

A) Scanning electron microscopy (SEM) images showing AuNR-anti-NGAL conjugates uniformly adsorbed on a paper substrate. Inset at the top left shows photographs of the bare filter paper (left) and filter paper after adsorption of AuNR-NGAL antibody conjugates (right). Scale bar = 0.25 cm. Inset at the top right shows the higher magnification image of paper with AuNR-anti-NGAL conjugates. B) Extinction spectra of AuNR-anti-NGAL conjugates on the paper substrate before and after ZIF-8 film coating, after ZIF-8 film removal and after exposure to 2.5 μg/ml of NGAL. C) LSPR shift corresponding to each step shown in (B). D) Retained recognition capability of ZIF-8-coated IgG-anti-NGAL conjugates on paper substrates stored at room temperature and 60 °C for different durations. Error bars represent standard deviations from three independent samples.